Available online at www.sciencedirect.com
ScienceDirect
Ceramics International 36 (2010) 887–891
CERAMICS INTERNATIONAL
www.elsevier.com/locate/ceramint

Thermoelectric properties of layered $Ca_{3.95}RE_{0.05}Mn_3O_{10}$ compounds (RE = Ce, Nd, Sm, Eu, Gd, Dy)

S. Lemonnier [a,*], E. Guilmeau [a], C. Goupil [a], R. Funahashi [b], J.G. Noudem [a]

[a] CRISMAT-ENSICAEN, CNRS/UMR 6508, 6 Bd Maréchal Juin, 14050 CAEN Cedex 4, France
[b] National Institute of Advanced Industrial Science and Technology, Midorigaoka, Ikeda, Osaka 563-8577, Japan

Received 10 September 2008; received in revised form 3 July 2009; accepted 6 October 2009
Available online 13 November 2009

Abstract

In this work, polycrystalline samples of the substituted $n = 3$ Ruddlesden-Popper $Ca_{4-x}RE_xMn_3O_{10}$ phase were prepared by solid-state reaction (RE, rare earth = Ce, Nd, Sm, Eu, Gd, Dy). Single phased samples were synthesized for sintering times larger than 150 h at 1350 °C. Complete thermoelectric characterizations were performed from 5 to 390 K, in terms of electrical resistivity (ρ), Seebeck coefficient (S) and thermal conductivity (κ). As expected, the substitution of Ca by different rare earth elements leads to a significant modification of the thermoelectric properties. With substitution level as low as 1.25 at.%, a remarkable decrease of the electrical resistivity is observed. The influence of this cationic substitution on the thermal conductivity (κ), Seebeck coefficient (S), and the figure of merit ZT is also discussed. In this study, the best one reaches 5.8×10^{-3} at 300 K for the $Ca_{3.95}Eu_{0.05}Mn_3O_{10}$ composition, a value 6 times higher than the ZT exhibited by the beginning $Ca_4Mn_3O_{10}$ sample.

Keywords: Oxides; Thermoelectric; Resistivity; Seebeck

1. Introduction

Nowadays, the thermoelectricity is known for its environmental interest. Indeed, thermoelectric generators can convert waste heat into electric energy without using moving parts and without producing carbon dioxide gas, toxic substances or other emissions. It is expected that thermoelectric power generation can provide a new energy source from the conversion of waste heat emitted by automobiles, factories, and other similar sources. For this purpose, oxide materials are potential candidates for a wide range of high temperature applications due to their high chemical stability and the absence of harmful elements in their compositions. Since the discovery of large thermoelectricity in Na_xCoO_2 [1], enthusiastic efforts have been devoted to explore new oxides exhibiting high thermoelectric performances, and some layered cobaltites, such as $[Ca_2CoO_3][CoO_2]_{1.62}$ and $[Bi_{0.87}SrO_2]_2[CoO_2]_{1.82}$ were found to exhibit interesting thermoelectric (TE) properties [2–4]. These p-type materials present large thermopower (>100 μV/K at 300 K), a relatively low electrical resistivity (∼1–10 mΩ cm at 300 K), and are expected to be incorporated in thermoelectric modules. More recently, theoretical predictions lead interest to focus on low dimensional materials with a ZT of 2.4 in Nb-doped $SrTiO_3$ thin films due to giant Seebeck coefficient in the superlattices [5]. On the other hand, the intensive investigations on n-type oxides are still going on because of their lower performances compared to p-type materials. Some potential n-type oxide candidates, like Ge-doped In_2O_3 [6], Al-doped ZnO [7], $LaNiO_3$ [8], $LaCoO_3$ [9] or $CaMnO_3$ [10] have been reported. Among these n-type materials, the perovskite $CaMnO_3$-based compound has been intensively studied due to its relatively low electrical resistivity and high Seebeck coefficient [11–15]. The decrease in the electrical resistivity by the means of cationic substitutions in the "A" site, like in $R_{1-x}A_xMnO_3$ [13] (R: rare earth cation, A: divalent cation such as Ca, Sr, Ba, Pb), $La_{1-x}Sr_xMnO_3$ [14], $Ca_{1-x}Dy_xMnO_{2.98}$ [16], $Ca_{1-x}La_xMnO_3$ [17], or in the "B" site, like in $CaMn_{1-x}Ru_xO_{3-\delta}$ [18,19], $AMn_{1-x}Mo_xO_3$ [19–21] results from the adoption of a mixed-valence oxidation state by Mn (Mn^{3+}/Mn^{4+}) which modifies the carrier concentrations and mobilities. Due to their low cost and promising TE properties, manganites were also used as potential candidates for n-type

* Corresponding author. Tel.: +33 2 31 45 13 67; fax: +33 2 31 45 13 09.
E-mail address: jacques.noudem@ensicaen.fr (S. Lemonnier).

0272-8842/$36.00
doi:10.1016/j.ceramint.2009.11.004

legs in thermoelectric modules [22,23]. On the other hand, reports [24,25] related to some layered manganites have been published showing that the $n = 3$ Ruddlesden-Popper system, corresponding to the $Ca_4Mn_3O_{10}$ compound, shows high Seebeck coefficient value of $-295\ \mu V/K$ and electrical resistivity of 200 mΩ cm at 300 K. In these compounds, the electrical resistivity should be highly reduced if texturing processes and optimized doping can be achieved. For example, Ce^{4+} for Ca substitution in $Ca_{4-x}Ce_xMn_3O_{10}$ has been studied [25] on polycrystalline samples with an enhancement of the thermoelectric performances. The induced reduction of Mn^{4+} to Mn^{3+} leads to a sharp decrease of the electrical resistivity down to 40 mΩ cm at 300 K with a moderate decrease of the absolute value of the Seebeck coefficient [24]. In this context, we prepared $Ca_{3.95}RE_{0.05}Mn_3O_{10}$ samples with different RE cationic substitutions and investigated their thermoelectric properties.

2. Experimental

Polycrystalline samples with nominal composition $Ca_{3.95}Sm_{0.05}Mn_3O_{10}$ (RE = Ce, Nd, Sm, Eu, Gd, Dy) were prepared by solid-state reaction using stoichiometric mixtures of $CaCO_3$, MnO_2 and RE oxide powders. The powders were mixed by ball-milling and calcined during 24 h under air at 900 °C. After calcination, the powders were ground and pelletized (Ø = 24 mm) under an uniaxial pressure of 100 MPa. The sintering temperature was fixed at 1350 °C during 2, 12, 24, 50, 100 and 150 h respectively in air. After this heat treatment, samples were cut in rectangular bars of 2 mm × 2 mm × 10 mm. The phase purity and composition was systematically checked by X-ray diffraction (XRD) using a PHILIPS PW1830 diffractometer with Cu Kα radiation. Microstructural observations were investigated with a ZEISS Supra 55 scanning electron microscope (SEM) coupled to energy dispersive spectroscopy (EDS) analyses in order to verify the cationic compositions. All the samples were polished and etched in air at 950 °C for 3 min in order to reveal the grain boundaries and microstructures.

Electrical resistivity measurements were carried out from room temperature to 10 K using the four probe method with a Quantum Design Physical Properties Measurement System (PPMS). Thermoelectric power and thermal conductivity measurements were performed from 320 to 5 K with an experimental setup described elsewhere [12].

3. Results and discussion

Fig. 1(a) and (b) show the different XRD patterns of undoped $Ca_4Mn_3O_{10}$ compound according to various sintering times (from 2 to 150 h). It can be observed that the single phase is obtained for dwell times higher than 100 h. The closer view of the 2θ range from 16° to 22° evidences more clearly the presence of the $Ca_3Mn_2O_7$ phase when the sintering time is

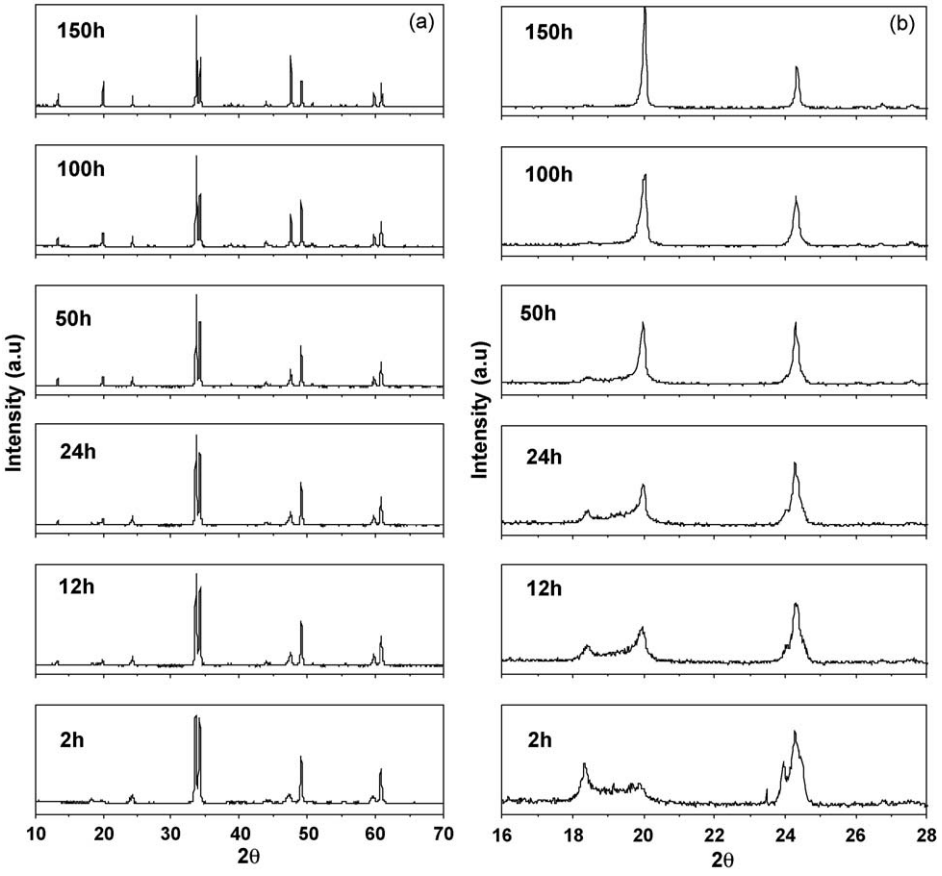

Fig. 1. (a) XRD patterns according to the sintering dwell time of the $Ca_4Mn_3O_{10}$ compound. (b) XRD patterns with a closer view (2θ range = 16–22°).

lower than 100 h, whose the corresponding peak intensity decreases as the sintering time increases. Moreover, the width of the $Ca_4Mn_3O_{10}$ diffraction peaks tends to be narrower as the sintering time increases, which tends to indicate an improvement of the phase crystallinity and an increase of the grain size. The evolution of the microstructure, shown in Fig. 2(a)–(f), indicates that the increase in the sintering dwell time is correlated with the formation and the increase in size of plate-like grains. It falls in agreement with the layered structure which can be described as single perovskite layers alternating with single rock-salt layers [26].

According to the XRD and SEM results, all the $Ca_{4-x}RE_xMn_3O_{10}$ compositions were sintered at 1350 °C for 150 h. The XRD patterns (not shown here) evidenced the high purity of the RE-substituted samples. The compositions of the substituted samples were also investigated by EDS analyses on individual grains and are reported in Table 1. The small deficit (around 1.6 at.%) in Mn cations probably originates from the volatilization of this latter at high temperature. The microstructure observations of the samples in the series $Ca_{4-x}RE_xMn_3O_{10}$ are similar to the parent $Ca_4Mn_3O_{10}$, indicating that the substitution of Ca by RE, which occurs in

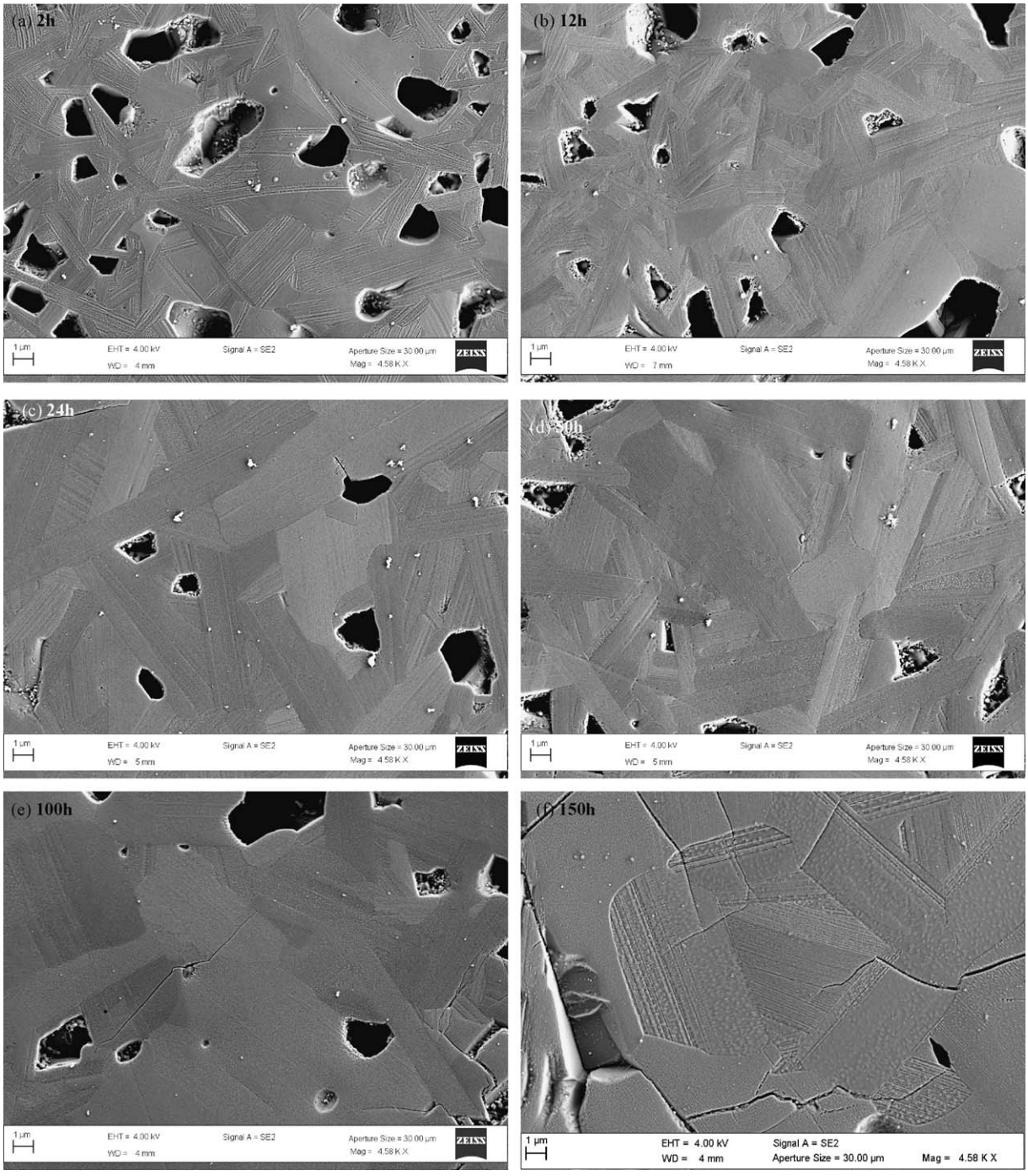

Fig. 2. SEM microstructures for different sintering times. (a) 2 h, (b) 12 h, (c) 24 h, (d) 50 h, (e) 100 h and (f) 150 h.

Table 1
EDS cationic ratio in the series $Ca_{3.95}RE_{0.05}Mn_3O_{10}$.

Nominal composition $Ca_{4-x}RE_xMn_3O_{10}$	EDS cationic ratio		
	Ca	Mn	RE
Ce	3.95	2.97	0.051
Nd	3.95	2.92	0.052
Sm	3.95	2.97	0.050
Eu	3.95	3.00	0.053
Gd	3.95	2.95	0.058
Dy	3.95	2.95	0.054

the perovskite-type layers, does not significantly modify the grains growth. The apparent densities of the sintered bulk materials are over than 90% of the theoretical density (4.34 g cm^{-3}).

The electrical resistivity (ρ) versus temperature curves of the different substituted samples are plotted in Fig. 3. All the samples exhibit a semiconducting behavior, *i.e.* $d\rho/dT < 0$, between 5 and 400 K. The substituted samples become more electrically conducting due to an expected increasing electron-carrier density through the partial substitution of RE^{4+} (Ce) or RE^{3+} (Nd, Sm, Eu, Gd and Dy) for Ca^{2+}. The resistivity of the undoped sample is equal to 1260 mΩ cm at 300 K which is higher than those reported elsewhere [26,27]. Lowest resistivity values around 30 mΩ cm were obtained for the Ce, Sm or Eu substituted samples with $x = 0.05$. These values are lower than those obtained for Ce-substitution by Zhou et al. [25] who measured 62 mΩ cm for $x = 0.045$ and 50 mΩ cm for the $x = 0.06$ compound at 300 K. These differences are probably linked to the oxygen content and/or Mn non-stoichiometry, in reason of the Mn volatilization during the sintering process.

The temperature dependence of the Seebeck coefficient (S) of all the RE-substituted ($Ca_{3.95}RE_{0.05}Mn_3O_{10}$) and parent ($Ca_4Mn_3O_{10}$) samples is shown in Fig. 4(a) and (b). We can clearly note that all the samples are n-type thermoelectric material across the entire temperature range. As foreseen, the substitution has for effect to considerably reduce the Seebeck coefficient, from −345 μV/K for the $Ca_4Mn_3O_{10}$ phase to about −140 μV/K for the RE-substituted samples at 300 K.

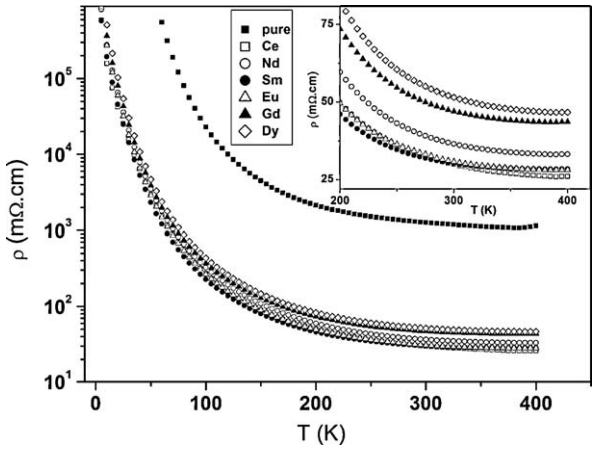

Fig. 3. Temperature dependence of the electrical resistivity in the series $Ca_{3.95}RE_{0.05}Mn_3O_{10}$. The inset shows a closer view from 200 K to room temperature.

The value of the Seebeck coefficient for the undoped compound is higher than the values reported by Lago et al. who obtained −295 μV/K at room temperature [24]. This result confirms the electrical resistivity measurements and tends to indicate that the carrier density may be affected by the oxygen content and/or Mn non-stoichiometry, as discussed above.

To finalize thermoelectric characterizations, thermal conductivity measurements were carried out from 5 to 320 K. The curves of κ evolution versus temperature are presented in Fig. 5. One can notice that the behaviors are different from the parent to the doped compounds. The first one presents a decreasing evolution with increasing temperature and reaches a value of 2.8 W m^{-1} K^{-1} at 300 K. The others compounds reach values between 1.5 and 4 W m^{-1} K^{-1} at 300 K showing a growing behavior with T. The lowest value of the series is obtained for the $Ca_{3.95}Dy_{0.05}Mn_3O_{10}$ compound with a thermal conductivity of 1.55 W m^{-1} K^{-1} at 300 K.

The Figure-of-Merit values at 300 K, defined as $ZT = S^2T/\rho\kappa$, (where S is the Seebeck coefficient, ρ the electrical resistivity and κ the thermal conductivity) are summarized in Table 2. The Eu-based composition shows better performances

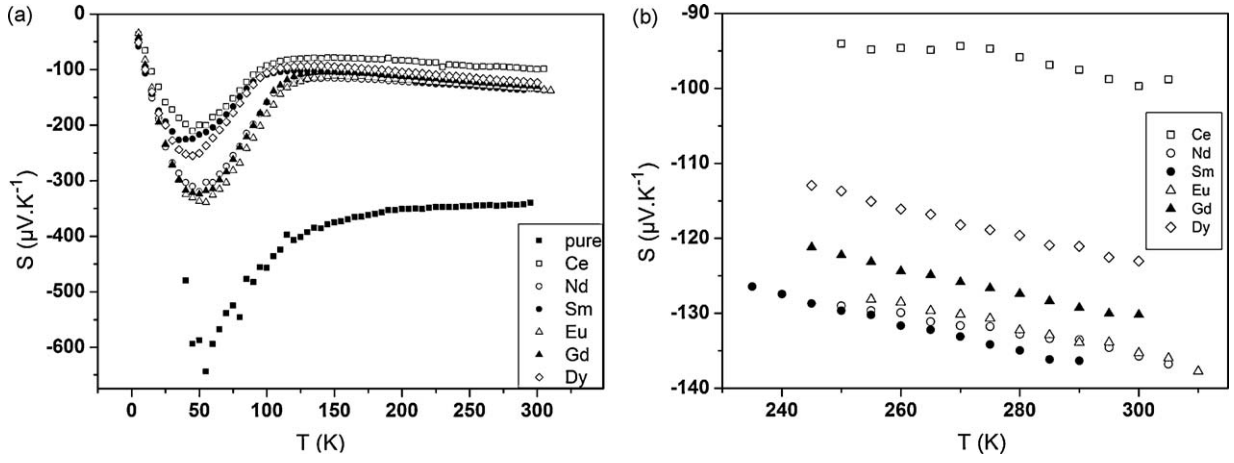

Fig. 4. (a) Temperature dependence of the Seebeck coefficient in the series $Ca_{3.95}RE_{0.05}Mn_3O_{10}$. (b) Closer view from 200 to 300 K of the Seebeck coefficient versus temperature curves in the series $Ca_{3.95}RE_{0.05}Mn_3O_{10}$.

Table 2
Seebeck coefficient, thermal conductivity, electrical resistivity and ZT values in the $Ca_{3.95}RE_{0.05}Mn_3O_{10}$ series at 300 K.

	Pure	Ce	Nd	Sm	Eu	Gd	Dy
S ($\mu V\ K^{-1}$)	−340	−100	−136	−139	−135	−130	−123
λ ($W\ m^{-1}\ K^{-1}$)	2.8	2.37	3.49	3.66	2.93	3.95	1.55
ρ (mΩ cm)	1255	29.85	36.47	30.2	30.7	46.9	51.4
ZT (300 K) ($\times 10^{-3}$)	0.98	3.91	4.09	4.94	5.83	2.64	5.38

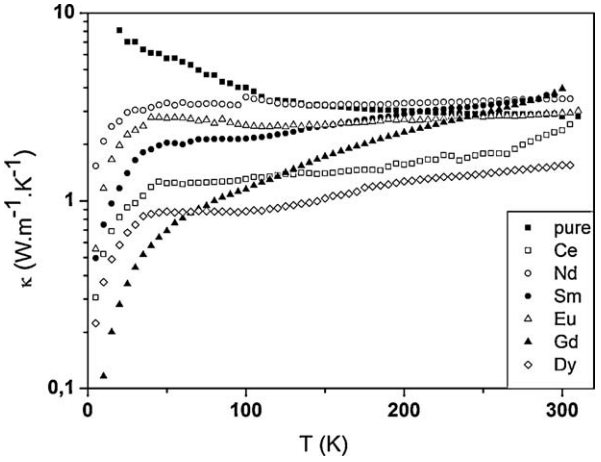

Fig. 5. Thermal conductivity versus temperature curves in the $Ca_{3.95}RE_{0.05}Mn_3O_{10}$ series.

than the other samples, with a resistivity of 31.5 mΩ cm, a Seebeck coefficient of −134 μV/K and a thermal conductivity of 2.93 $W\ m^{-1}\ K^{-1}$ at 300 K. The calculated ZT reaches 5.8×10^{-3} at this temperature which is 6 times higher than the ZT of the pure $Ca_4Mn_3O_{10}$ sample. Furthermore, one can notice that the lowest electrical resistivity value is obtained for the Ce^{4+}-doped as predicted due to the RE highest valence value implying a higher carrier concentration.

Unfortunately, no relation between the RE ionic radii and the TE properties was clearly established. Further investigations and experiments are still needed.

4. Conclusion

Thermoelectric properties of the $Ca_{3.95}RE_{0.05}Mn_3O_{10}$ compounds were studied. The rare earth substitution on the Ca site was checked by X-ray diffraction and EDS analysis. This substitution leads to an increase in carrier concentration in n-type thermoelectric materials and to reduce both electrical resistivity (ρ) and Seebeck coefficient (S). The Eu-based composition presents an electrical resistivity and a Seebeck coefficient respectively of, 40 times and 2.5 times lower than the $Ca_4Mn_3O_{10}$ material, and a similar value of thermal conductivity, resulting in an improvement of the ZT value by a factor 6. These thermoelectric properties are of course far from the best values reported in the literature on other oxide systems. However an optimization of the formulation and doping, coupled to a preferential orientation between grains, *e.g.* by texturing, should improve significantly the thermoelectric performances of these manganites.

Acknowledgment

SL acknowledges a fellowship from ‘‘French Ministère de la Recherche et de la Technologie’’.

References

[1] I. Terasaki, Y. Sasago, K. Uchinokura, Phys. Rev. B 56 (1997) R12685.
[2] R. Funahashi, I. Matsubara, H. Ikuta, T. Takeuchi, U. Mizutani, S. Sodeoka, Jpn. J. Appl. Phys. 39 (2000) L1127.
[3] A.C. Masset, C. Michel, A. Maignan, M. Hervieu, O. Toulemonde, F. Studer, B. Raveau, J. Hejtmanek, Phys. Rev. B 62 (2000) 166.
[4] H. Leligny, D. Grebille, O. Perez, A.C. Masset, M. Hervieu, B. Raveau, Acta Crystallogr. B 56 (2000) 173.
[5] H. Ohta, et al. Nat. Mater. 6 (2007) 129.
[6] D. Bérardan, E. Guilmeau, A. Maignan, B. Raveau, Solid State Commun. 146 (2008) 97.
[7] M. Ohtaki, T. Tsubota, K. Egushi, H. Arai, J. Appl. Phys. 79 (1996) 1816.
[8] R. Funahashi, S. Urata, T. Kouuchi, M. Mikami, 22nd Int. Conf. Thermoelectr. Proc., La Grande Motte, 184 (2003).
[9] S. Hébert, D. Flahaut, C. Martin, S. Lemonnier, J. Noudem, C. Goupil, A. Maignan, Jiri Hejtmanek, Prog. Solid State Chem. 35 (2–4) (2007) 457.
[10] M. Ohtaki, H. Koga, T. Tokunaga, K. Eguchi, H. Arai, J. Solid State Chem. 120 (1995) 105.
[11] A. Maignan, C. Martin, F. Damay, B. Raveau, J. Hejtmanek, Phys. Rev. B 58 (1998) 2758.
[12] J. Hejtmanek, Z. Jirak, M. Marysko, C. Martin, A. Maignan, M. hervieu, B. Raveau, Phys. Rev. B 60 (1999) 14057.
[13] A. Urushibara, Y. Moritomo, T. Arima, A. Asamitsu, G. Kido, Y. Tokura, Phys. Rev. B 51 (1995) 14103.
[14] C.N.R. Rao, A.K. Cheetham, R. Mahesh, Chem. Mater. 8 (1996) 2421.
[15] A. Maignan, C. Martin, F. Damay, B. Raveau, Chem. Mater. 10 (1998) 950.
[16] P.X. Thao, T. Tsuji, M. Hashida, Y. Yamamura, J. Ceram. Soc. Jpn. 11 (2003) 544.
[17] B. Fisher, L. Platagan, G.M. Reisner, A. Knizhnik, Phys. Rev. B 61 (2000) 470.
[18] Y. Zhou, I. Matsubara, R. Funahashi, G. Xu, M. Shikano, Mater. Res. Bull. 38 (2003) 341.
[19] L. Pi, S. Hébert, C. Martin, A. Maignan, B. Raveau, Phys. Rev. B 67 (2003) 024430.
[20] M. Miclau, S. Hébert, R. Retoux, C. Martin, Solid State Chem. 178 (2005) 1104.
[21] A. Maignan, S. Hébert, L. Pi, D. Pelloquin, C. Martin, C. Michel, M. Hervieu, B. Raveau, Cryst. Eng. 5 (2002) 365.
[22] I. Matsubara, R. Funahasi, T. Takeuchi, T. Shimizu, K. Ueno, S. Sodeoka, Appl. Phys. Lett. 78 (23) (2001) 3627.
[23] E.S. Reddy, J.G. Noudem, S. Hébert, C. Goupil, J. Phys. D: Appl. Phys. 38 (2005) 3751.
[24] J. Lago, P.D. Battle, M.J. Rosseinsky, J. Phys.: Condens. Matter 15 (2003) 6817.
[25] Y. Zhou, I. Matsubara, R. Funahashi, G. Xu, M. Shikano, Mater. Res. Bull. 37 (2002) 1123.
[26] A.I. Mihut, L.E. Spring, R.I. Bewley, S.J. Blundell, W. Hayest, T. Jestadt, B.W. Lovett, R. Mcdonald, F.L. Pratt, J. Singleton, P.D. Battle, J. Lago, M.J. Rosseinsky, J.F. Vente, J. Phys.: Condens. Matter 10 (1998) L727.
[27] I.D. Fawcett, J.E. Sunstrom IV, M. Greenblatt, M. Croft, K.V. Ramanujachary, Chem. Mater. 10 (1998) 3643.